Asymmetric solitons in saturable nonlinear medium with complex potential

F. C. Moreira[1], S. B. Cavalcanti[1]
[1] *Universidade Federal de Alagoas, Campus A. C. Simões - Av. Lourival Melo Mota,*
s/n, Cidade Universitária, Maceió - AL 57072-900, Brazil
(Dated: June 8, 2020)

We study the stability of soliton waves through saturable nonlinear inhomogeneous media with gain and loss, not necessarily in balance. We report on the existence of families of stable asymmetric spatial solitons in a saturable nonlinear medium in the presence of a gain/loss asymmetrical profile. A tunable parameter defines the deviation from the $\mathcal{PT}$-symmetric case, and a thorough study on the existence and stability of soliton families is carried out. The properties of the nonlinear modes bifurcating from the eigenvalue of the underlying linear problem are investigated. The eigenvalue ranges in the power-eigenvalue diagrams for different gain/loss profile are inspected. We find that the saturable nonlinearity severely restricts these ranges as the eigenvalues tend quite fast to an asymptotic profile, as power increases. The examples of the dynamics of the asymmetric solitons obtained by numerical simulations exhibit a good agreement with the analytical results.

PACS numbers: 42.65.Tg, 42.65.Sf

I. INTRODUCTION

The past decade has witnessed an intense activity in linear optical systems, described by non-Hermitian Hamiltonians, triggered by reports on a wide class of complex potentials that obeys the parity-temporal symmetry, the well known $\mathcal{PT}$ symmetry [1]. These $\mathcal{PT}$-symmetric Hamiltonians exhibit real spectra even though non-Hermitian, as it has been demonstrated in seminal works within a quantum context [2, 3]. However, these Hamiltonians are quite suitable to describe $\mathcal{PT}$-symmetric optical structures, through the association of the local potential function with complex-valued refractive index profiles. This association has been quite fruitful and has turned the field of optics and photonics to be a particularly adequate ground to test the amazing consequences of $\mathcal{PT}$-symmetric systems. Actually, $\mathcal{PT}$ symmetry was investigated theoretically and firstly demonstrated experimentally in the optical context [4–7]. The inclusion of gain/loss in nonlinear propagation is an even more interesting problem, particularly, in the case of the nonlinear Schrödinger equation. Based on the non-integrable character of the nonlinear Schrödinger equation, Wadati has demonstrated that a system where $\mathcal{PT}$ symmetry is modeled by a refractive index having a symmetric real part and an anti-symmetric imaginary one, admits soliton propagation [8]. This notion developed into a wide class of $\mathcal{PT}$- symmetric as well as non-$\mathcal{PT}$-symmetric potentials with real spectra. In the linear theory such modes were studied for exactly integrable models in [9, 10], and their nonlinear extension were reported in [11]. Similarly, these classes of potentials have been investigated within the context of the Gross-Pitaewskii equation [12]. Recent reviews on the matter may be found in Refs. [13–15]. Various types of nonlinearities have been investigated: solitons in $\mathcal{PT}$-symmetric localized potentials with second-harmonic generation were investigated in [16] and was found that such system admits stable solitons above the $\mathcal{PT}$-symmetric phase breaking threshold; gap solitons in one-dimensional $\mathcal{PT}$ -symmetric periodic potentials with saturable nonlinearity have also been reported in Refs. [17, 18]. Furthermore, a logarithmically saturable nonlinearity investigation indicated the existence of stable solitons in $\mathcal{PT}$ - symmetric periodic potentials [19]. Quite recently an investigation on the fundamental and higher-order families of solitons in one dimension, in the presence of a $\mathcal{PT}$-symmetric potential and a saturable nonlinearity, concluded that by increasing the saturation parameter one may partly hinder the instability of these solitons [20, 21].

The developments reported in $\mathcal{PT}$-symmetric optical structures have also triggered further studies to include non-$\mathcal{PT}$-symmetric complex potential functions in various contexts widening the potentiality of features such as a real spectra as well as a phase transition [22–24]. Several classes of non-$\mathcal{PT}$-symmetric complex potentials of the Wadati type with real spectra have been suggested [25]. These potentials contain free parameters that represent tuning. By tuning the refractive index below a critical value the spectrum undergoes a complex phase transition. By adding a real part with an adjustable parameter one opens an additional tunable possibility with ranges that admit real spectra and also a phase transition to the complex phase. Nonlinear Kerr systems have been studied in a non-$\mathcal{PT}$-symmetric potential and stable soliton solutions were found [26]. In Ref. [27] the existence of continuous families of nonlinear modes in a complex asymmetric potential are attributed to an underlying conserved quantity in the system's dynamics. Based on this fact, the existence and stability of solitons in quadratic nonlinear unidimensional media under the influence of a one-parameter family (an asymmetric class of Wadati potential) have also been studied [30]. Families of stable solitons bifurcating from the fundamental mode, as well as from the second harmonic, were reported. Materials with high nonlinear coefficients such as semiconductor doped glasses and organic polymers, cannot be described by a Kerr-type nonlinearity [28], as in these materials, the saturation of the nonlinear refractive index occurs at moderately high pulse intensities, so that one must study the effect of higher order nonlinearities. Asymmetric solitons due to the symmetry breaking phase transition have been studied in a saturable medium [29]. However, to the best of our knowledge, a saturable nonlinearity in non-$\mathcal{PT}$-symmetric potentials have not been under investigation. Furthermore, theoretical and experimental results have indicated that a saturable nonlinear medium is suitable for the propagation and control of spatial solitons. As a notorious example photorefractive optical solitons, which can be induced at relatively low power formation, are quite important for applications in all-optical switching and signal processing [31]. Therefore, in this paper we propose an asymmetric potential to describe the existence and the stability properties of solitons in a saturable nonlinear medium. Our main objective in this work is to include an asymmetry parameter to see whether one may attain a flexibility with respect to the balance between nonlinearity and asymmetry that stabilizes the soliton. In this way we hope to extend the class of potential functions, manipulating, saturation, gain and loss, to achieve new functionalities. This paper is organized as follows. In Section II the theoretical model is described. Section III briefly presents the linear properties of the potential function. The stability and dynamics of the localized solutions are considered in Section VI.

II. THEORETICAL MODEL

Let us begin by writing the propagation equation of an optical field $u(\xi,\zeta)$ through a diffractive nonlinear saturable medium:

$$i\frac{\partial u}{\partial \zeta}+\frac{\partial^2 u}{\partial \xi^2}+\left[g^2+\alpha g+ig_\xi\right]u+\sigma\frac{|u|^2}{1+\gamma|u|^2}u=0 \quad (1)$$

u being the dimensionless amplitude of the field while ξ and ζ are, respectively, dimensionless transverse and propagation coordinates, scaled to the characteristic size of a localized modulation of the refractive index, which is fully described by a real function $g \equiv g(\xi)$. The real part being $g^2+\alpha g$, where α is a free parameter which plays the role of a relative strength of the real part of the potential to the imaginary part, which is defined as: $g_\xi \equiv \frac{dg}{d\xi}$. This adjustable parameter α, widens the scope of non-Hermitian Hamiltonians with real spectra and may drive the system to a phase transition to the complex plane [25]. Fig. 1 shows the variation of the real part $g^2+\alpha g$ as a function of α illustrating its effect on the amplitude of the real part of the potential function. The last term in equation (1) represents a saturable third order nonlinear material with saturation parameter γ. The case $\gamma=0$ represents the usual Kerr nonlinearity without saturation. The nonlinearity may be of a self-focusing ($\sigma>0$) or a self-defocusing type ($\sigma<0$).

We look for localized solutions of (1) in the form,

$$u\left(\xi,\zeta\right)=w\left(\xi\right)e^{ib\zeta},, \quad (2)$$

where b is the soliton propagation constant and $w(\xi)$ is the solution of

$$\frac{d^2w}{d\xi^2}+\left[g^2+\alpha g+ig_\xi-b\right]w+\sigma\frac{|w|^2}{1+\gamma|w|^2}w, \quad (3)$$

constrained to zero boundary conditions, that is, $w\left(\xi\right)\to 0$ as $|\xi|\to\infty$.

III. LINEAR PROPERTIES OF THE ASYMMETRIC LOCALIZED POTENTIAL

Previous work [25] has shown that, similarly to the $\mathcal{PT}$-symmetric case, the complex potential

$$G(\xi,\alpha)=g^2+\alpha g+ig_\xi \quad (4)$$

when substituted into the linear version of equation (3),

$$Lw=b_1 w, \quad (5)$$

where b_1 is the linear eigenvalue and the operator L is defined as

$$L=\frac{d^2}{d\xi^2}+G, \quad (6)$$

depending on the value of α, may exhibit all-real spectrum. Furthermore it was proved that, for sufficiently mild conditions the value $\alpha=0$ always guarantees a real spectrum for (6). Let us now briefly describe the recently reported [30] linear properties of (6) when the potential G is generated by the following function:

$$g=V\,\mathrm{sech}\left[\left(1+\frac{\beta+\beta\tanh(\xi)}{2}\right)\xi\right], \quad (7)$$

where the constant V is the amplitude and the parameter β represents its degree of asymmetry. The function g is continuously differentiable, has a global maximum at $\xi=0$ and is asymmetric for $\beta\neq 0$, as is illustrated in Fig. 1. The function g decays as e^{ξ} when $\xi\to-\infty$ and $e^{-|1+\beta|\xi}$ when $\xi\to\infty$. In Fig. 1 we show the spectrum of (6) using (7) for different values of α and a fixed $\beta=-0.5$. A complex phase transition is found for $\alpha<\alpha_{cr}=-0.187$, where a pair of complex eigenvalues emerge due to the collision of two localized eigenvalues at $b_1=0.013$ (See Fig. 1). Note that for $\alpha>0$ there are no phase transitions, just the appearance of additional localized modes due to the higher amplitude of G. Here, in contrast with the symmetric system for which $\beta=0$, there are no degenerated discrete eigenvalues as there is no symmetry to induce degeneracy. Instead, as α changes continuously, a complex phase may appear only due to the collision of simple discrete modes

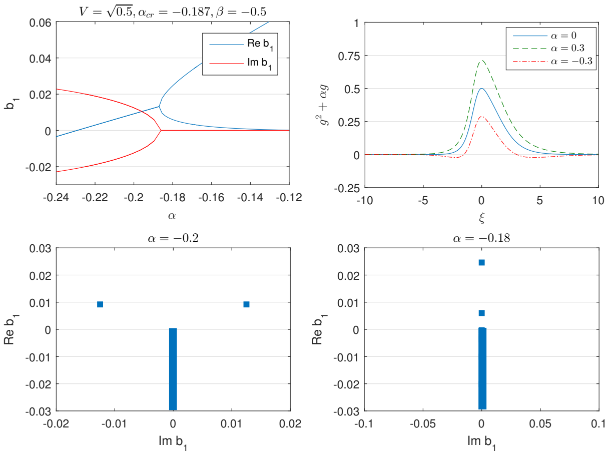

FIG. 1: Upper left panel shows the eigenvalues of (6) with $V = 0.5$, $\beta = -0.5$ as a function of the parameter α. Upper right panel shows the effect of α on the shape of the real part of the potential G. Lower panels show the eigenvalues below ($\alpha = -0.18$) and above ($\alpha = -0.2$) the phase transition, where the real spectrum breaks into a complex phase. Note the appearance of a complex pair of eigenvalues due to the collision of two real valued eigenvalues at $b = 0.013$ where $\alpha_{cr} = -0.187$ (not shown). The spectrum contains an imaginary pair for $\alpha < \alpha_{cr}$.

as illustrated in Fig. 1. Albeit shown here for the specific case of $\beta = -0.5$, different values of β are found to exhibit the same behavior with respect to the breaking of the real valued phase of the spectrum. The effect of different values of the asymmetry parameter β on the eigenvalues b_1 is shown in Fig. 2. In all results presented below, we have chosen the values $V = \pm\sqrt{0.5}$. Note in (7) that this means that the absolute value of the amplitude of g is fixed, so that only the decay rate of the $\xi > 0$ region is modified. This affects the values of b_1: as β decreases, the area of g becomes larger and, consequently, the number of localized modes increases. Clearly if $\beta = -1$, then

$$\lim_{\xi \to -\infty} G(\xi) = 0, \tag{8a}$$

$$\lim_{\xi \to \infty} G(\xi) = V^2 + \alpha V. \tag{8b}$$

This is an interesting situation as for $\beta = -1$ the potential G becomes very similar to a Heaviside step function with some localized imaginary part while the spectrum approaches a continuous band defined by $b_1 \leq V^2 + \alpha V$.

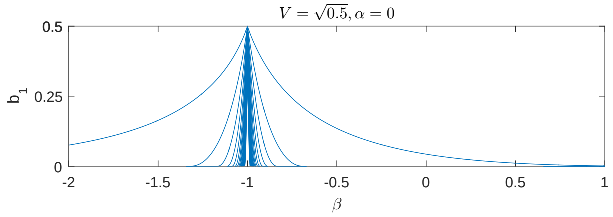

FIG. 2: Discrete spectrum of b_1 as a function of β. Note the appeareance of a continuous band at $\beta = -1$. The values chosen for the potential are $V = \sqrt{0.5}$ and $\alpha = 0$.

IV. NONLINEAR LOCALIZED MODES AND LINEAR STABILITY ANALYSIS

Let us now, investigate the existence and stability of the localized solutions of (3). From now on we restrict our considerations mainly to solutions bifurcating from the linear limit, more specifically, as $w \to 0$, b tends to a finite eigenmode of the linear problem i.e., $b \to b_1$. The total energy P of a localized solution is defined by:

$$P = \int_{\infty}^{\infty} |w|^2 \, d\xi. \tag{9}$$

Let us now perturb the solution $u(\xi, \zeta)$ by writing:

$$u(\xi, \zeta) = \left(w(\xi) + p_+(\xi) e^{-i\lambda\zeta} + \overline{p}_-(\xi) e^{i\overline{\lambda}\zeta} \right) e^{ib\zeta}, \tag{10}$$

where, $|p_\pm(\xi)| \ll 1$, represents small perturbations. Inserting (10) into (1) and collecting linear terms in $p_\pm(\xi)$ one ends up with an eigenvalue problem given by:

$$L_s \begin{pmatrix} p_+ \\ p_- \end{pmatrix} = \lambda \begin{pmatrix} p_+ \\ p_- \end{pmatrix}, \tag{11a}$$

$$L_s = \begin{pmatrix} L - b + \sigma \frac{|w|^2(\gamma|w|^2+2)}{(1+\gamma|w|^2)^2} & \sigma \frac{w^2}{(1+\gamma|w|^2)^2} \\ -\sigma \frac{\overline{w}^2}{(1+\gamma|w|^2)^2} & -\overline{L} + b - \sigma \frac{|w|^2(\gamma|w|^2+2)}{(1+\gamma|w|^2)^2} \end{pmatrix} \tag{11b}$$

so that, whenever an eigenvalue λ with $\mathrm{Im}(\lambda) > 0$ occurs the solution is linearly unstable.

A. Effects of saturation parameter γ

Investigating the effect of the saturation parameter γ we have found that all investigated branches with $\gamma > 0$ exhibit a vertical asymptote in the (b, P) plane as shown in Fig. 3 and Fig. 4.

This is expected since for solutions with very high intensities one has,

$$\lim_{|w(\xi)|^2 \to \infty} \sigma \frac{|w(\xi)|^2}{1 + \gamma |w(\xi)|^2} = \frac{\sigma}{\gamma} \tag{12}$$

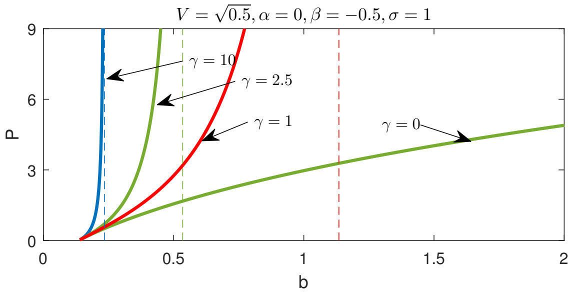

FIG. 3: Total energy P as a function of b with $V=\sqrt{0.5}$, $\beta=-0.5$, $\sigma=1$ and different values of the saturation constant γ. Dashed lines represents the asymptotes $b_1+\sigma/\gamma$. All solutions are stable.

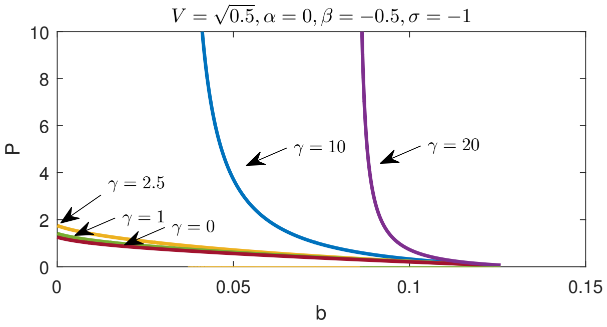

FIG. 4: Total energy P as a function of b with $V=\sqrt{0.5}$, $\beta=-0.5$, $\sigma=-1$ and various values of the saturation constant γ. All solutions are stable.

Now, inserting (12) in (3) we obtain

$$\frac{d^2w}{d\xi^2}+\left[g^2+\alpha g+ig_\xi-b+\frac{\sigma}{\gamma}\right]w, \tag{13}$$

which, of course the same as (5)

$$Lw=(b-\frac{\sigma}{\gamma})w \tag{14}$$

and has a localized mode at $b=b_1+\frac{\sigma}{\gamma}$, where b_1 is a discrete value of (5). In other words, as the amplitude of the soliton increases its profile becomes similar to the shape of the linear eigenmode it bifurcated from, in the limit $w\to 0$.

In fact, extensive numerical calculations of branches show that the fundamental branches exist in the region $b\in\left(b_1, b_1+\gamma^{-1}\right)$ for the $\sigma=1$ case and $b\in\left(b_1-\gamma^{-1}, b_1\right)$ when $\sigma=-1$. Interestingly enough as, using the fact that the branch must be localized within the region between b_1 and $b_1+\frac{\sigma}{\gamma}$, one realizes that the $\sigma=1(\sigma=-1)$ branch bifurcates to the right(left).

In what concerns stability, we have investigated two main potential functions, i.e., $G(\xi)$ and $G^*(\xi)$ which correspond to the cases $V=\sqrt{0.5}$ and $V=-\sqrt{0.5}$ respectively, if one also substitutes $\alpha\to-\alpha$. It should be noted here that, if w is a solution of (3) with G then clearly w^*

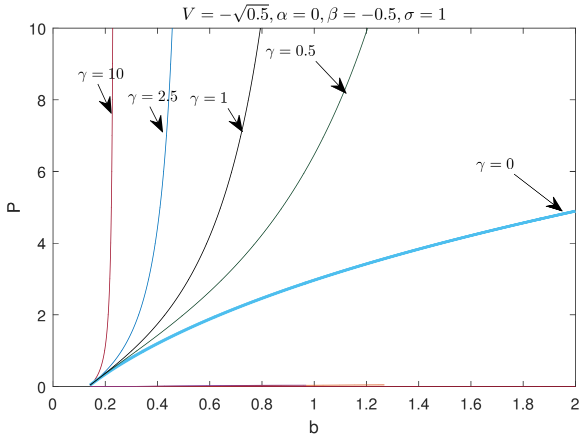

FIG. 5: Total energy P as a function of b with $V=-\sqrt{0.5}$, $\beta=-0.5$, $\sigma=1$ and for various values of saturation constant γ. Right panel shows an expanded view of the region where the transition between stable and unstable solutions occurs. Thick lines represent linearly stable solutions and lines represent unstable solutions.

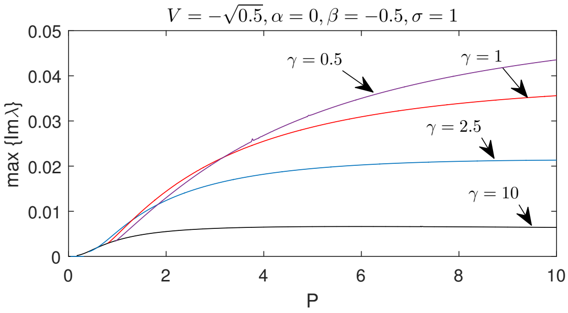

FIG. 6: Maximum value of imaginary part of (11) as a function of the total energy of localized modes P for several values of γ. Note that all branches are unstable but $\max\{\mathrm{Im}\lambda\}\to\lambda_\gamma$ as $P\to\infty$. The higher the value of γ, the lower the value of λ_γ. Parameters are $V=-\sqrt{0.5}$, $\beta=-0.5$, $\sigma=1$.

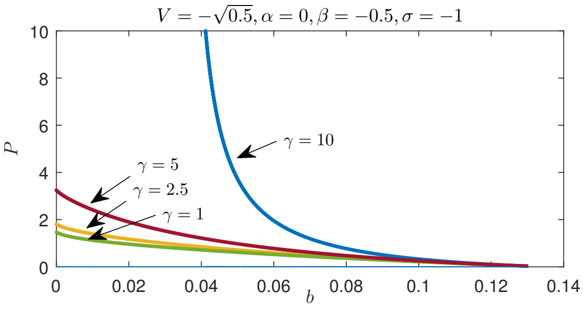

FIG. 7: Total energy P as a function of b with $V=-\sqrt{0.5}$, $\beta=-0.5$, $\sigma=-1$ and different values of saturation constant γ. All solutions are stable.

is a solution of (3) with G^*, and both solutions are obtained for the same value of P. Despite no difference in the $(b, P)-$curve, the stability scenario of the solutions is completely different in each case, as we demonstrate below. First we choose $V = \sqrt{0.5}$. In both cases, $\sigma = \pm 1$, no linearly unstable solutions were obtained, at least for moderately high amplitude solutions with $P \sim 10$ as is displayed in Fig. 3 and Fig. 4.

With respect to the $V = -\sqrt{0.5}$ case, we have found only unstable solutions in the $\sigma = 1$ case as depicted in Fig. 5. The instability here appears due to an asymmetric internal mode that bifurcates from the continuous spectrum of (11), at $\lambda = \pm b$. This internal mode appears as soon as $P > 0$, thus there are no stable solutions because this mode moves to the $\mathrm{Im}\lambda > 0$ region. Note that this instability rate is quite low when $|b - b_1| \ll 1$. The Fig. 6 clearly shows that branches with higher values of γ tend to present a lower degree of instability in this case. In the $V = -\sqrt{0.5}$ case we have found stable solutions only in the case of the defocusing nonlinearity, $\sigma = -1$ as is shown in Fig. 7.

B. Effects of asymetry parameter β

The effect of different values of the asymmetry constant β has also been investigated. We have studied all four combinations of $V = \pm\sqrt{0.5}$ and $\sigma = \pm 1$. See in Fig. 8 and Fig. 9 the case $V = \sqrt{0.5}$. The effect of β in both $\sigma = \pm 1$ cases is to shift b_1 closer to $b_1 = 0.5$ as expected, with more discrete modes appearing as $\beta \to -1$ (See Fig. 2). The vertical asymptote $b = b_1 + \sigma/\gamma$ is still present in the branches. Regarding stability, no changes were observed: all solutions were found to be stable in the $V = \sqrt{0.5}$ case as illustrated in Fig. 8 and Fig. 9. Solutions with $V = -\sqrt{0.5}$ are stable for $\sigma = -1$ (See Fig. 10) and all solutions are unstable in the $\sigma = 1$ case (See Fig. 11).

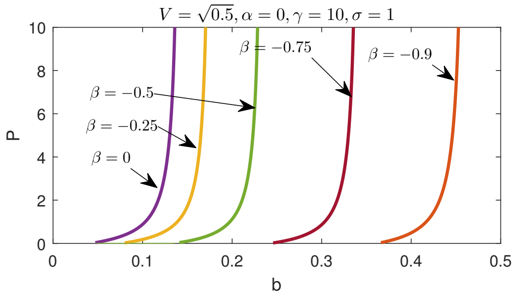

FIG. 8: Total energy P as a function of b with $V = \sqrt{0.5}$, $\beta = -0.5$, $\sigma = 1$ and different values of saturation constant γ. All solutions are stable.

Note that in both cases, $\sigma = \pm 1$, with $V = -\sqrt{0.5}$ there are stable solutions only if $\beta = 0$, i.e., the $\mathcal{PT}$-symmetric case. In Fig. 12 one may see that, in fact $\max\{\mathrm{Im}\lambda\} \to 0$ as $\beta \to 0$.

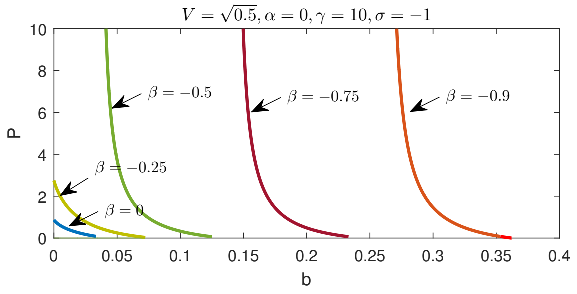

FIG. 9: Total energy P as a function of b with $V = \sqrt{0.5}$, $\gamma = 10$, $\sigma = -1$ and several values of saturation constant γ. All solutions are stable.

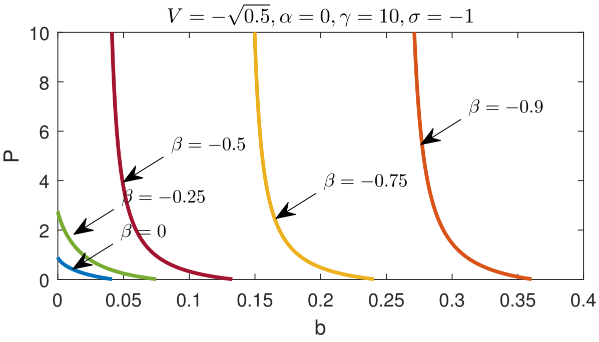

FIG. 10: Total energy P as a function of b with $V = -\sqrt{0.5}$, $\gamma = 10$, $\sigma = -1$ and various values of asymmetry constant β. All solutions are stable.

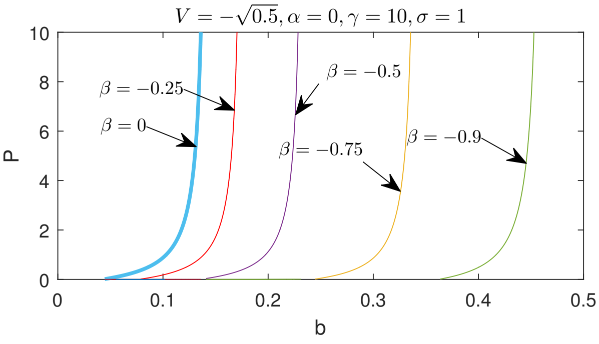

FIG. 11: Total energy P as a function of b with $V = -\sqrt{0.5}$, $\gamma = 10$, $\sigma = 1$ and different values of asymmetry constant β. All solutions are stable.

C. Investigation of gain and loss parameter α

Here we fix $\beta = -0.5$, $\gamma = 10$ and change α to investigate its effects on the existence and stability of fundamental branches. The first case to be investigated is the one with $V = \sqrt{0.5}$ and $\sigma = 1$ and we turn to Fig. 13, from where one may conclude that all observed solutions are stable. The second case with $V = \sqrt{0.5}$

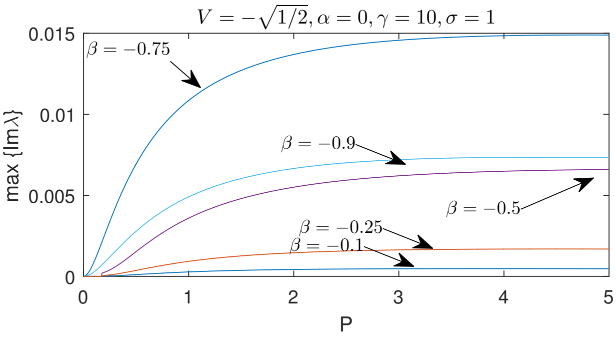

FIG. 12: Maximum value of the imaginary part of (11) as a function of total energy of localized modes P. Note that all $\beta < 0$ branches are unstable but $\max\{\mathrm{Im}\lambda\} \to 0$ as $\beta \to 0$. Parameters are $V = -\sqrt{0.5}$, $\gamma = 10$, $\sigma = 1$.

and $\sigma = -1$ shows that an unstable region may exist above some threshold in P if $\alpha < 0$ is close enough to α_{cr}. The stable region becomes smaller as α gets closer to α_{cr}, eventually disappearing along with the branch itself when $\alpha \to \alpha_{cr}$. Next, for $V = -\sqrt{0.5}$ and $\sigma = 1$. we note that there are no stable solutions. Finally, for $V = -\sqrt{0.5}$ and $\sigma = -1$, all solutions are stable.

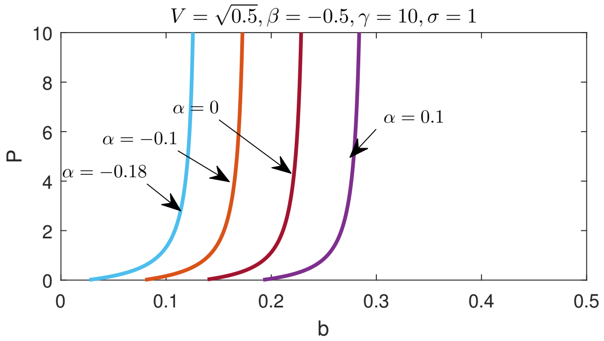

FIG. 13: Total energy P as a function of b with $V = \sqrt{0.5}$, $\gamma = 10$, $\sigma = 1$ and various values of α. All solutions are stable.

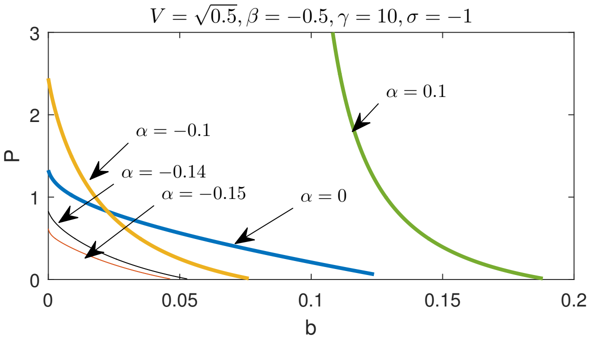

FIG. 14: Total energy P as a function of b with $V = \sqrt{0.5}$, $\gamma = 10$, $\sigma = -1$ and several values of α. Thick lines (lines) represent linearly stable (unstable) solutions.

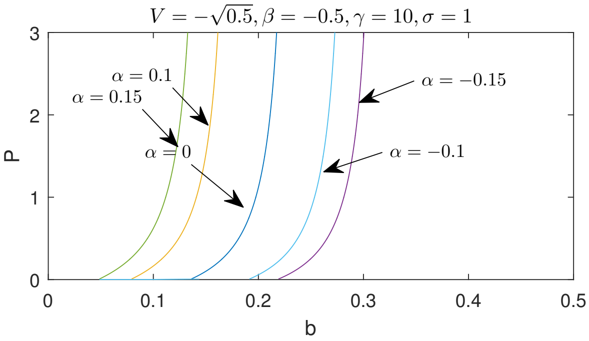

FIG. 15: Total energy P as a function of b with $V = -\sqrt{0.5}$, $\gamma = 10$, $\sigma = 1$ and different values of α. All solutions are unstable.

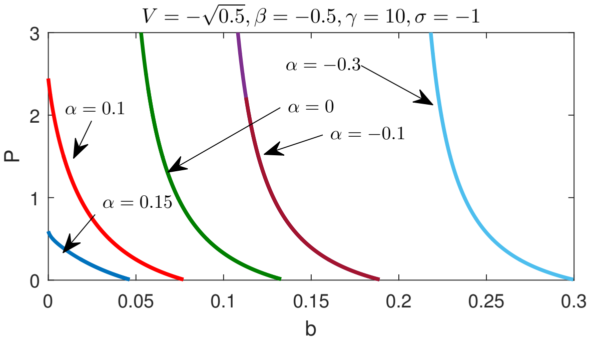

FIG. 16: Total energy P as a function of b with $V = -\sqrt{0.5}$, $\gamma = 10$, $\sigma = 1$ and different values of asymmetry constant β. All solutions are stable.

V. DYNAMICS OF LOCALIZED SOLUTIONS

To corroborate the results described in the last section, in this section we proceed to make comparisons between the model of perturbations (11) and direct propagation of (3) using the solutions found as initial conditions in

(1). In all propagations we have added a 1% of noise to the amplitude at $\zeta = 0$. Here our objective is to show that the linear stability analysis predicts quite well the evolution of localized modes under weak perturbations.

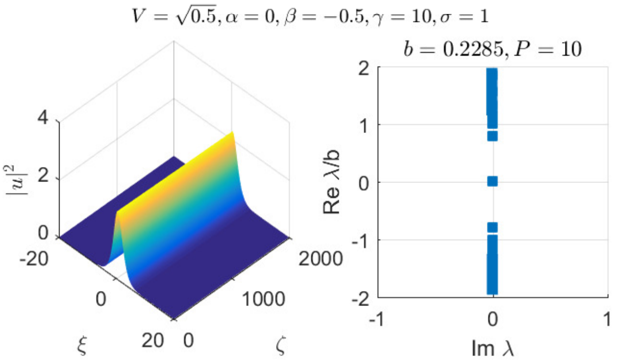

FIG. 17: (Color online)(Left panel) Intensity $|u|^2$ during propagation of a high power $P = 10$ stable soliton with $b = 0.23$. (Right panel) Corresponding eigenvalues of (11). Parameters are $V = \sqrt{0.5}, \beta = -0.5, \alpha = 0, \gamma = 10$ and $\sigma = 1$.

The first property that we have observed is the stability of three, among four possible combinations of signals of V and σ, three cases: $V = \sqrt{0.5}$ and $\sigma = \pm 1; V = -\sqrt{0.5}$ and $\sigma = -1$, exhibit stable solutions as possible to see in Fig. 17 and Fig. 18 for the $V = \sqrt{0.5}$ and $\sigma = 1$ case. In all figures of dynamics we have used $\gamma = 10$ as it does not change the existence or absence of stable solutions. Note that the discrete modes of stable solitons with $\beta \neq 0$ tends to the negative imaginary part of the plane, differently from the $\beta = 0$ case, where the discrete modes of stable solitons must have Im$\lambda = 0$ as it is depicted in Fig. 18 .

In Fig. 19 we show two examples of unstable solutions in the branch with $\alpha = -0.14$ $\beta = -0.5$. Note that while β does not change by itself the stability properties of the solutions when all other parameters are fixed, the parameter $\alpha < 0$ may in fact introduce instability in the system, both of oscillatory (complex λ) and purely exponentially decaying (purely complex λ) types, as displayed in Fig. 19. Dynamics of unstable propagation in case $V = -\sqrt{0.5}$ and $\sigma = 1$ is shown Fig. 20. Finally in Fig. 21 illustrates the dynamics of a stable solution in the case $V = -\sqrt{0.5}$ and $\sigma = -1$.

Looking at the stability spectrum of (11), one may conclude that the role of the sign of V has with respect to the stability of branches may be understood by considering that non-$\mathcal{PT}$-symmetric cases, i.e., $\beta \neq 0$, do not possess the symmetry $\lambda = \lambda^*$ as expected. So, one may find discrete eigenvalues λ in either Im$\lambda > 0$ or Im$\lambda < 0$ regions. Now, if one inspects a branch where the potential is substituted as $G \to G^*$, the spectrum of (11) changes to $\lambda \to \lambda^*$, as all terms other than L are real in L_s. Thus, whenever a stable solution exists with some Im$\lambda < 0$ for a given G, there is an unstable solution in the branch of the system with the potential G^*. There are cases where changing G for G^* does not change the stability of a function. This happens solely when a stable solution has Im$\lambda = 0$ as possible to see in Fig. 17 and Fig. 21 for example.

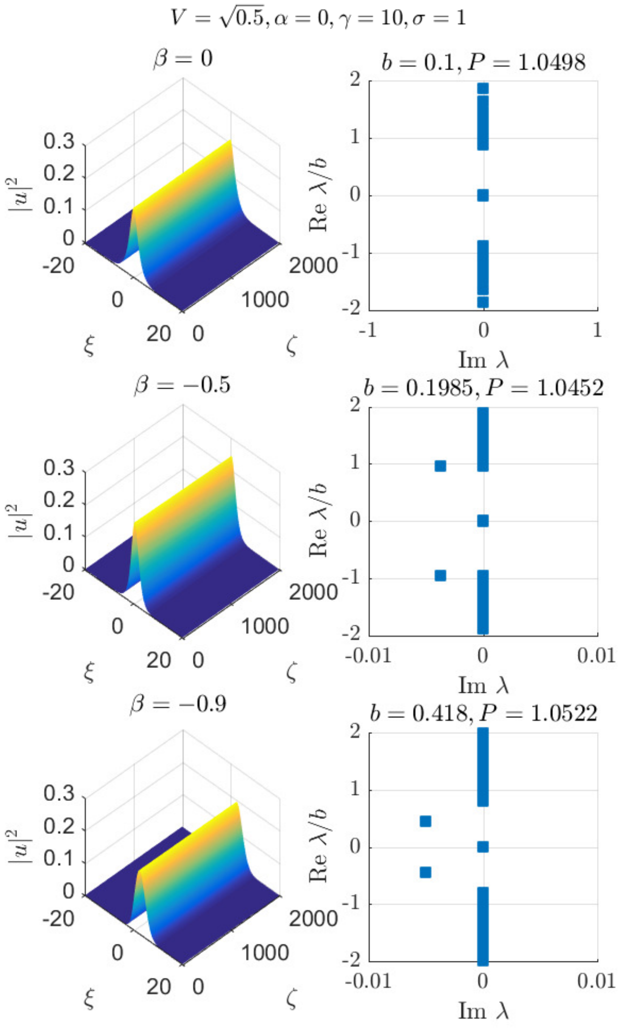

FIG. 18: (Color online)(Left panels) Intensities $|u|^2$ during propagation of stable solutions of branches with different values of the asymetry constant β. Parameters are $V = \sqrt{0.5}, \alpha = 0, \gamma = 10$ and $\sigma = 1$.

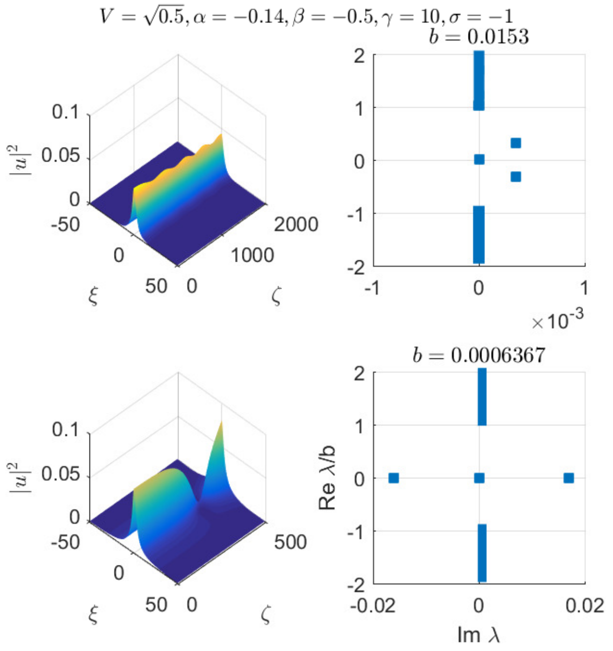

FIG. 19: (Color online)(Left panels) A Intensities $|u|^2$ during propagation of unstable solutions. (Right panels) Corresponding eigenvalues of (11) Note the that de linear stability model correctly predicts the onset of a oscillatory instability in the solution with $b = 0.0153$ and the exponential decay in the case $b = 0.0006367$. Parameters are $V = \sqrt{0.5}, \beta = -0.5, \alpha = -0.14, \gamma = 10$ and $\sigma = -1$.

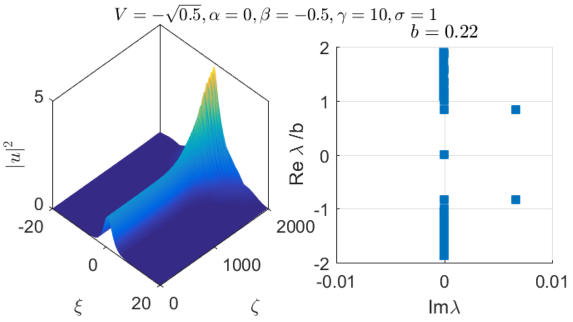

FIG. 20: (Color online)(Left panel) Intensitt $|u|^2$ during propagation of an unstable solution. (Right panel) Corresponding eigenvalues of (11). Note that the linear stability model correctly predicts the onset of a oscillatory instability. Also note that the instability develops quite slowly. Parameters are $V = -\sqrt{0.5}, \beta = -0.5, \alpha = 0, \gamma = 10$ and $\sigma = 1$.

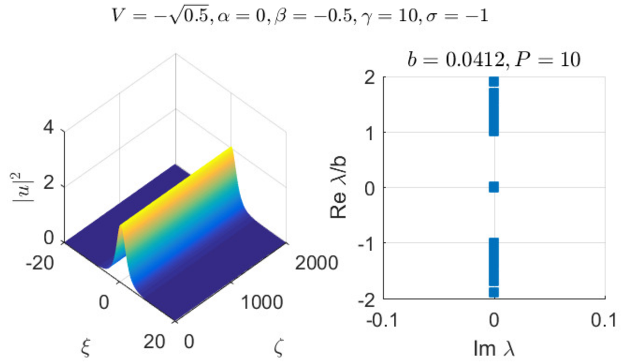

FIG. 21: (Color online)(Left panel) Intensity $|u|^2$ during propagation for a high power, $P = 10$, stable solution with $b = 0.0412$. Parameters are $V = -\sqrt{0.5}, \beta = -0.5, \alpha = 0, \gamma = 10$ and $\sigma = -1$.

VI. CONCLUSIONS

Summing up, we have studied the existence and stability properties of soliton families in media with a saturable nonlinearity in a non-$\mathcal{PT}$-symmetric complex refractive index. We have found the unexpected result that such media does support the existence of asymmetric solitons in both self-focusing as well self-defocusing case. Furthermore, all branches of solitons found to bifurcate from the linear limit in case the saturation parameter $\gamma \neq 0$, exhibit a vertical asymptote in the power-eigenvalue diagram, revealing that γ restricts the range where localized modes are supported. Also, the asymptotic value of b for large powers is uniquely determined by the saturation parameter and this value decreases for higher γ driving the system to a less unstable situation. This result is similar to the result reported in $\mathcal{PT}$-symmetric optical lattices [?]. Furthermore, as the amplitude of the soliton increases its profile becomes similar to the shape of the linear eigenmode from where it was originated. In case of positive V we find stable solitons in both media, i.e., under the effect of self-focusing or self-defocusing. In cases where V takes on negative values we find that, when it comes to the stability properties these are complete altered and all solutions become unstable in the self-focusing media, i.e., for $\sigma = 1$.

Acknowledgments

The authors grateful acknowledge the partial financial support from the Brazilian agencies, CNPq and Capes.

---

[1] C. M. Bender and S. Boettcher, Phys.Rev.Lett. **80**, 5243 (1998).

[2] C. M. Bender, S. Boettcher, and P. N. Meisinger, J. Math. Phys. **40**(5), 2201?2229 (1999).

[3] C. M. Bender, D. C. Brody, and H. F. Jones, Phys. Rev. Lett. **89**(27), 270401 (2002).

[4] R. El-Ganainy, K. G. Makris, D. N. Christodoulides, and Z. H. Musslimani, ?Optical P T-symmetric structures,? Opt. Lett. **32**(17), 2632?2634 (2007).

[5] A. Ruschaupt, F. Delgado and J. G. Muga, J. Phys. A **38** L171 (2005).

[6] A. Guo, G. J. Salamo, D. Duchesne, R. Morandotti, M. Volatier-Ravat, V. Aimez, G. A. Siviloglou, and D. N. Christodoulides, Phys. Rev. Lett. **103**(9), 093902 (2009).

[7] C. E. Rüter, K. G. Makris, R. El-Ganainy, D. N. Christodoulides, M. Segev, and D. Kip, Nat. Phys. **6**, 192 (2010).

[8] M. Wadati, J. Phys. Soc. Jpn. **77**, 074005 (2008).

[9] M. Znojil, J.Phys. A Math. Gen. **33**, L61 (2000).

[10] Z. Ahmed, Phys. Lett. A **282**, 343-348 (2001).

[11] Z. H. Musslimani, K. G. Makris, R. El-Ganainy, and D. N. Christodoulides Phys. Rev. Lett. **100**, 030402, (2008).

[12] I. V. Barashenkov, D. A. Zezyulin and V. V. Konotop, in Non-Hermitian Hamiltonians in Quantum Physics. F. Bagarello, R. Passante, and C. Trapani, Eds. Springer Proceedings in Physics, **184**, 143 (2016).

[13] Konotop VV, Yang J, Zezyulin DA. Rev. Mod. Phys.**88**, 035002 (2016).

[14] Suchkov SV, Sukhorukov AA, Huang J, Dmitriev SV, Lee C, Kivshar YS, Laser and Photonics Reviews **10**, 177-213 (2016).

[15] El-Ganainy R, Makris KG, Khajavikhan M, Musslimani ZH, Rotter S, Christodoulides DN. Nature Physics **14**, 11-19 (2018).

[16] F. C. Moreira, F. Kh. Abdullaev, V. V. Konotop, and A. V. Yulin, Phys. Rev. A **86**, 053815 (2012).

[17] Cao P, Zhu X, He Y, Li HG. Opt. Commun. **316**, 190-197 (2014).

[18] Li L, Li H, Lai T. Opt. Commun. **349**, 171-179.

[19] Zhu X, Li H, Eur. Phys. J. D **70**, 14 (2016).

[20] P. Li, D. Mihalache, and B. A. Malomed, arXiv:1804.03314v1, [physics.optics] (2018).

[21] P. Li, C. Dai, R. Li, and Y. Gao, Optics Express **26**, 6949 (2018).

[22] F. Cannata, G. Junker, and J. Trost, Phys. Lett. A **246**,219226 (1998).

[23] M.A. Miri, M. Heinrich, and D. N. Christodoulides, Phys. Rev. A **87**, 043819 (2013).

[24] E.N. Tsoy, I.M. Allayarov and F. Kh. Abdullaev, Opt. Lett. **39**, 42154218 (2014).

[25] S. Nixon and J. Yang, Phys. Rev. A **93**(3), 031802 (2016).

[26] E. N. Tsoy, I. M. Allayarov, and F. Kh. Abdullaev, Opt. Lett. **39**, 4215 (2014); V. V. Konotop and D. A. Zezyulin, Opt. Lett. **39**, 5535 (2014).

[27] D. A. Zezyulin and V.V. Konotop, Phys. Rev. Lett. **108**, 213906 (2012).

[28] S. Gatz and J. Herrmann, J. Opt. Soc. Am. B **8**, 2296-2302 (1991).

[29] P. Li, C. Dai, R. Li, and Y. Gao, Optics Express **26**, 6949 (2018).

[30] F. C. Moreira and S. B. Cavalcanti, Phys. Rev. A **94**, 043818 (2016).

[31] M. Segev, B. Crosignani, A. Yariv and B. Fischer, Phys. Rev. Lett. **68**, 923 (1992).